

Rb-Sr and Sm-Nd ISOTOPIC STUDIES OF SHERGOTTITE Y980459 AND A PETROGENETIC LINK BETWEEN DEPLETED SHERGOTTITES AND NAKHLITES. C.-Y. Shih¹, L. E. Nyquist¹, H. Wiesmann¹ and K. Misawa³, ¹Mail Code C23, Lockheed-Martin Space Operations, 2400 NASA Parkway, P.O. Box 58561, Houston, TX 77258-8561, chi-yu.shih1@jsc.nasa.gov, ²Mail Code SR, NASA Johnson Space Center, 2101 NASA Parkway, Houston, TX 77058, l.nyquist@jsc.nasa.gov, ³NIPR, Tokyo, Japan, misawa@nipr.ac.jp.

Introduction: Y980459 was found near the Mian-Yamato Nunataks, Antarctica in 1998 and was recently classified as an olivine-bearing shergottite [1]. It petrographically resembles many other olivine-phyric shergottites mostly found in hot deserts, e.g. DaG476/489, SaU005/094, Dohfar 019, NWA 1068/1110, NWA 1195 and EETA 79001 lith. A [e.g. 2, 3]. However, Y980459 is unique among these meteorites in several respects. It is apparently very fresh and only weakly shocked. Also, it completely lacks plagioclase, but contains abundant residual volcanic glass [e.g. 4]. This group of olivine-phyric shergottites is characterized by variable crystallization ages from ~172 Ma to ~575 Ma and ejection ages from ~1 Ma to ~20 Ma [e.g. 5]. They probably represent volcanic melts originated from the deep Martian mantle. We performed Rb-Sr and Sm-Nd isotopic analyses on Y980459 to determine its crystallization age and compared its age and isotopic signatures with those obtained from other olivine-phyric shergottites and QUE 94201, the other Antarctic olivine-free shergottite. QUE 94201 and some olivine-phyric shergottites e.g. DaG, SaU, Doh and EETA lith A have similar depleted-LREE patterns and are herein referred to as *depleted shergottites*. A petrogenetic model correlating depleted shergottites and nakhlites is also proposed. Preliminary Rb-Sr and Sm-Nd isotopic data for Y980459 were presented earlier at the NIPR, Japan, in 2003 [6].

Samples: A sample of Y980459 weighing ~1.5 g was allocated, and an aliquant sample weighing ~0.5 g was used for this study. The fine-grained sample containing yellow/brown olivine megacrysts was processed initially by gently crushing and removing olivine megacrysts. Then the sample was further crushed to grain size <149 μm . The bulk rock sample (WR) was taken before the rest of the sample was further crushed and sieved into two size fractions, 149-74 μm and <74 μm . Mineral separations were made from the finer <74 μm fraction by density separation using heavy liquids of bromoform, methylene iodide and Clerici's solutions. At $\rho > 3.45 \text{ g/cm}^3$, we obtained a good yellow/brown olivine (Ol) sample of >95% purity. At $\rho = 3.32\text{--}3.45 \text{ g/cm}^3$ and $\rho = 2.85\text{--}3.32 \text{ g/cm}^3$, we obtained white pyroxene-rich (Px) and black glass-rich (Gl) samples, respectively. A very small mesostasis-rich sample (~0.8 mg) was obtained at $\rho < 2.85 \text{ g/cm}^3$. In order to eliminate possible terrestrial contaminants, WR, Px, and Gl samples were washed by 2N HCl with sonication. Ol and $\rho < 2.85 \text{ g/cm}^3$ samples were washed with less concentrated 0.5N HCl. Both the residues (r) and leaches (l) of these samples plus an unwashed WR sample were analyzed for Rb, Sr, Sm, and Nd following the chemi-

cal procedures and using Finnigan-MAT mass spectrometers, either 261 or 262, multi-collector instruments [7].

Rb-Sr isotopic results: The $^{87}\text{Rb}/^{86}\text{Sr}$ and $^{87}\text{Sr}/^{86}\text{Sr}$ data for two unwashed WR, two acid-washed WR and three acid-washed minerals (Gl, Px and $\rho < 2.85 \text{ g/cm}^3$) from Y980459 are shown in Fig 1. These seven samples, plus four leachates and acid-washed olivine samples (not shown), do not define a linear array, indicating that the Rb-Sr isotopic system was "open" and has been disturbed by terrestrial contamination. Two unwashed WR and five acid-washed samples do form a linear array corresponding to a tie-line age of $296 \pm 90 \text{ Ma}$ for $\lambda(^{87}\text{Rb}) = 0.01402 \text{ Ga}^{-1}$ and $I(\text{Sr}) = 0.701485 \pm 0.000071$. Data for all seven samples lie $\leq \pm 1 \text{ } \epsilon\text{-unit}$ from the isochron. If this tie-line or isochron represents the age of Y980459, it is within the age limits obtained from the evolved olivine-free depleted shergottite QUE 94201 [8], but not within age limits for other olivine-phyric depleted shergottites. The distinctively lower $I(\text{Sr}) = 0.701298 \pm 14$ for QUE 94201 [8] suggests that Y980459 and QUE 94201 may represent two flows produced contemporaneously.

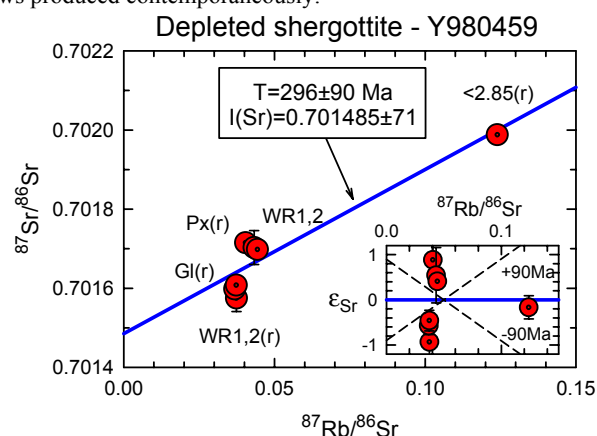


Figure 1. Rb-Sr isochron for Y980459.

Sm-Nd isotopic results: Fig. 2 shows $^{147}\text{Sm}/^{144}\text{Nd}$ and $^{143}\text{Nd}/^{144}\text{Nd}$ data of three bulk rock and three mineral (Px, Gl and Ol) samples for Y980459. One unwashed WR and three acid-washed WR, Gl and Px samples define a tie-line corresponding to age of $290 \pm 45 \text{ Ma}$ for $\lambda(^{87}\text{Rb}) = 0.00654 \text{ Ga}^{-1}$ and initial ϵ_{Nd} value $= +44.1 \pm 1.8$. This age is in good agreement with the Rb-Sr tie-line age of this rock and Rb-Sr and Sm-Nd ages of QUE94201 [8]. Y980459 is more closely related to QUE94201 than to the other olivine-phyric depleted shergottites. Two leachates and the Ol samples plot significantly below the tie-line and point towards the terrestrial aeolian

particulates of [9,10]. Our Sm-Nd isotopic data and high K and Br abundances in this rock reported recently [11] suggest that the meteorite may have exposed to terrestrial aerosol contamination.

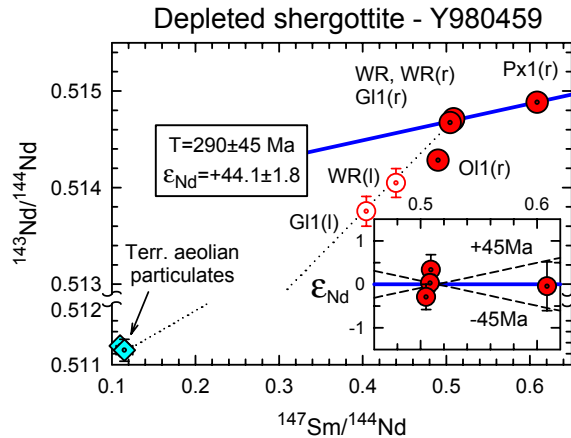


Figure 2. Sm-Nd isochron for Y980459.

REE pattern implications: Fig. 3 summarizes the CI-normalized REE distribution patterns of six depleted shergottites (QUE94201, Y980459, EETA lith A, Doh 019, DaG476 and SaU005) and five nakhlites (Nakhla, Lafayette, Governor Valadares, Y000593 and NWA 817) [12]. All depleted shergottites regardless of their olivine contents have similar highly LREE-depleted patterns. In contrast, all nakhlites have similar highly LREE-enriched patterns. These complementary REE patterns commonly observed in melt-residue pairs involving garnets are consistent with the interpretation that this melt-residue relationship probably exists between these two groups of rocks. In this scenario, nakhlites and depleted shergottites originated from a common mantle source. During partial melting events, nakhlites would be the early melts, which are enriched in LREE, whereas, depleted shergottites would be the solid residues depleted in LREE left after the prior extraction of melt components. Later melting of these depleted residues would have produced magmas parental to depleted shergottites. Similar ^{142}Nd excesses for depleted shergottites and nakhlites [e.g. 13,14] also suggest that they came from similar source regions.

A genetic link between depleted shergottites and nakhlites: Results of partial melting calculations of a garnet-bearing nakhlite source with $^{147}\text{Sm}/^{144}\text{Nd} = 0.235$ are illustrated in a conventional initial ϵ_{Nd} vs. age plot in Fig. 4. Present-day data for depleted shergottites and nakhlites are shown in solid symbols. Open symbols are their ϵ_{Nd} values at times of magma formation. Assuming that the nakhlite source is composed of garnet, Cpx and Ol, similar to the mineral composition of Martian mantle proposed by [15], and using the Sm and Nd garnet-melt partition coefficients of [16], the calculated $^{147}\text{Sm}/^{144}\text{Nd}$ for ~10% Cpx-rich melt have low values of ~0.14 that match well with those for nakhlites. The respective $^{147}\text{Sm}/^{144}\text{Nd}$ ratios for garnet-rich

residues have high values of ~0.44, similar to those of the depleted shergottites. Extensive melting of such residues, leaving most olivine in the residues, at later times ~300-600 Ma ago could produce magmas with garnet-like REE patterns which are parental to depleted shergottites.

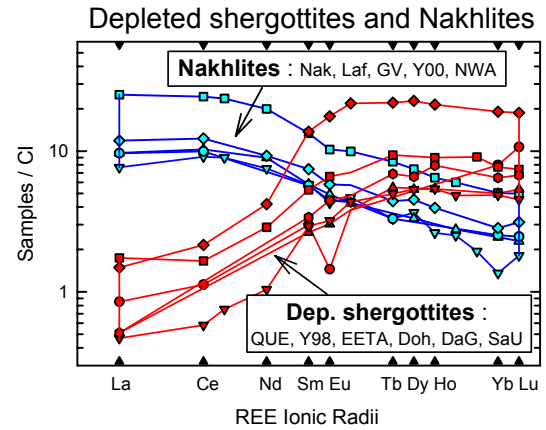


Figure 3. REE patterns for depleted shergottites and nakhlites.

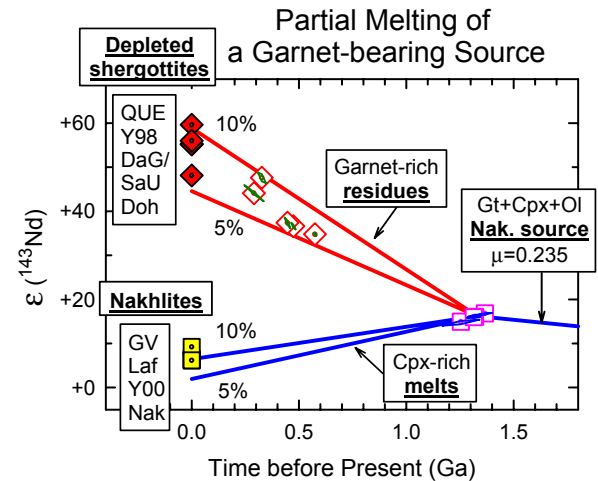


Figure 4. ϵ_{Nd} vs. T(age) for depleted shergottites and nakhlites.

References: [1] NIPR *Meteorite Newsletter* (2002) vol.1, no.11. [2] Goodrich C. (2002) *Met. Planet. Sci.* **37**, B31-B34. [3] Barrat A. et al. (2002) *GCA*, **66**, 3505-3518. [4] Greshake A. et al. (2003) *NIPR Symposium*, 29-30. [5] Nyquist L.E. et al. (2001) *Chronology and Evolution of Mars*, **96**, 105-164. Kluwer Academic Publ. Dordrecht/Boston/London. [6] Shih C.-Y. et al. (2003) *NIPR Symposium*, 125-126. [7] Nyquist L.E. et al. (1994) *Met. Planet. Sci.* **29**, 872-885. [8] Borg L. et al. (1997) *GCA*, **61**, 4915-4931. [9] Goldstein S.L. et al. (1984) *E&PSL*, **70**, 221-236. [10] Albarede F. & Brouxel M. (1987) *E&PSL*, **82**, 25-35. [11] Dreibus G. et al. (2003) *NIPR Symposium*, 19-20. [12] Meyer C., Jr (2003) *Mars Meteorite Compendium*, NASA JSC#27672. [13] Harper C., Jr., et al. (1996) *Science*, **267**, 213-217. [14] Jagoutz E. et al. (2003) *NIPR Symposium*, 47-48. [15] Bertka C.M. and Fei Y. (1997) *JGR*, **102**, 5251-5264. [16] Draper D.S. et al. (2002) *LPSC-XXXIII* (CD-ROM #1306).